PHYSICS

ANALYSIS

OVERVIEW

Analysis is crucial to scientific research as it is a means for researchers to show the accuracy and reliability of their obtained data. This chapter discusses numerical analysis, percent deviation, non-parametric test, and thermal analysis. The following methods describe how different analyses can be used to compare results and to screen relevant from irrelevant data. Analysis can also be done with equipment such as the thermogravimetric analyzer in this chapter.

A. Numerical

(Clement, Josue, Ledesma, Murga, Madriñan)

One of the two techniques for observing the Golden ratio in structures is numerical analysis, where the ratio of the different measurements of the structure under study is taken. In this study, a spreadsheet was used for the automation of calculations.

The analysis is carried out by dividing *a*, the greater length, to *b*, the lesser length given by the formula; ratio = $a/b \approx 1.6.1812297$. Subsequent calculations follow using the same basic idea of dividing the greater by the lesser. This is done on all lengths, widths, and areas with priority on locations where the Golden ratio is typically found eg. areas of facades or floor plans, lengths or distances of columns and arches.

B. Percent Deviation

(Clement, Josue, Ledesma, Murga, Madriñan)

Following the Golden ratio deliberately may lead to inconveniences in applying certain designs and adjustments should be made. Therefore in comparing the ratio to the golden ratio it was decided that the relevant ratios are those within 5% deviation from the golden ratio.

The percent deviation was calculated by getting the absolute value of:

$$\left(\frac{Dervied\ Ratio}{Golden\ Ratio} \times 100\right) - 100.$$

D. Non-Parametric Test

(Barrios, Cortez, Herman, Larroder, Yu Jeco, Watanabe, Okada)

The Wilcoxon Signed Ranks Test was used to compare the daily output power of both the convex and Fresnel setups. It is a non-parametric test used to compare matched samples to determine if a significant difference exists for their population mean ranks. This non-parametric test was used since the data is not entirely random due to the assigned time for gathering the values, and thus cannot be assumed to be normally distributed.

Average values for voltage, current, output power, irradiance, and temperature were obtained by averaging the values at each hour for the 3-day testing period.

E. Thermal Analysis

(Tukasim, Beñosa, Pe, Jolito)

The simultaneous Thermal Analyzer 8000 (STA 8000) is an equipment used in measuring the mass time change while controlling the temperature at 15°C-1600°C. The weight loss history and exothermic phenomenon of the individual blends in a linearly heated environment were studied using a thermal analyzer (PerkinElmer STA 8000) which is coupled with a differential scanning calorimetry (DSC) to measure the heat flow into or out of the sample over time. The thermal analysis was done at the University of the Philippines Visayas-Miag-ao Campus.

The Thermogravimetric analyzer (model: PerkinElmer Simultaneous Thermal Analyzer 8000) was used in the gasification process.

For each experiment, a sample weighing 20 mg was heated in a small furnace in the thermal analyzer to study its thermal degradation. The samples were heated from 20°C to 900°C at a heating rate of 50°C·min^{-1}. The samples were gasified at a temperature of 900°C, this was decided by basing on a study done by Patra and Sheth (2015) which states that the gasification of biomass is usually conducted between 800°C- 1000°C, to promote the different endothermic reactions that are occurring during gasification. In summary, a sample run typically contains five steps namely, isothermal step for stabilization, temperature ramp step to the drying temperature of 110°C, another isothermal step to fully remove the moisture content, another temperature ramp step to the desired gasification temperature, and Finally, another isothermal step where the gasification would take place. Table 5 shows the summary of the strides.

Table 5. *Running program inputted in STA 8000.*

Seg No.	Method	Description	Purpose
1	Isothermal	Heat for 2.0 min at 20°C	Mass stabilization
2	Temperature Ramp	Heat from 20°C to 110°C at 50°C/min	Increase temperature to the drying temperature
3	Isothermal	Hold for 4.0 min at 110°C	Removal of moisture
4	Temperature-Ramp	Heat from 110°C to 900°C at 50°C/min	Increase to the devolatilization, gasification, and combustion temperature
5	Isothermal	Hold for 10.0 min at 900°C	Devolatilization, gasification, and combustion

CALCULATION

OVERVIEW

Calculations often involve using standard equations in quantifying values of interest. This chapter discusses the quantification of gasification (conversion of biomass to fuel) reaction and the conversion efficiency of photovoltaic cells. The first study shows the use of previously established models to determine the most appropriate that can describe their experimental data. While the latter shows the calculations for the efficiency of photovoltaic cells and the measure of quality of the solar cell.

A. Gasification Reaction

(Tukasim, Beñosa, Pe, Jolito)

Co-gasification of biomass and coal is emerging as a potential clean fuel technology as it reduces greenhouse gas emissions, lowers gross power output, and increases thermal efficiency. The present study aimed to determine the potential of Theobroma cacao (UIT Variety) pod husks as an alternative to coal by investigating the gasification kinetics. After obtaining the mass time curve data from the thermal analysis it was then analyzed in order to determine the proximate composition. The proximate composition includes the percentage mass of moisture, volatile matter, fixed carbon, and ash content. As seen in Figure 17, the graph is subdivided into four different parts namely the removal of moisture and volatile matter, carbon dioxide gasification of char, and the combustion of the remaining char. The data were analyzed using a series of steps by determining the amount of moisture, volatile matter content, fixed carbon content, and the ash content of the sample that was being tested.

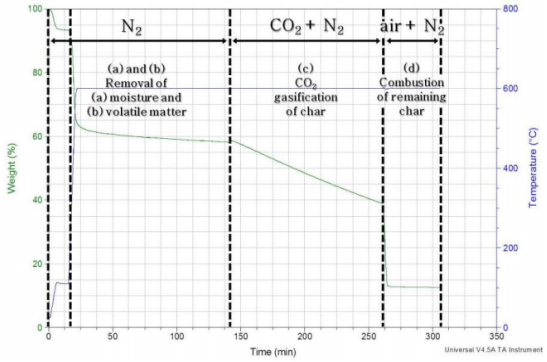

Figure 17. *Graph of char combustion.*

The evaluation was carried out by determining the fractional conversion using the equation below. This is done in order to determine the best model. After which, it was fitted into the gas solid reaction model.

$$X = \frac{W_0 - W}{W_0 - W_{ash}}$$

Where W_0 is the initial mass of the pre-gasified char, W_{ash} is the mass of ash in the primary char sample, and W is the mass of the char at any time t. (Massoudi Farid *et al*, 2016) The reaction rate of the gas solid models which are expressed as the carbon mass balance, Volumetric model and Shrinking Core model, were determined using the respective equations. The volumetric model is considered to be the simplest and straightforward model, while the Shrinking Core model is described to be solid molecule used or being consumed by either dissolution or through the chemical reactions happening.

$$X = 1 - e^{-k_{VM}t}$$

where k_{VM} is the first-order reaction rate constant and X is the fractional conversion of carbon.

$$X = 1 - (1 - k_{SCM}t)^3$$

where k_{scm} is the average reaction rate constant.

As for the Random Pore model, there is another step to go through before determining the rate constant. The surface parameter will be first determined, it was used to determine the rate constant. The Random Pore model considers the growth of pores and the coalescence of these pores which causes a reduction of area through a combination of overlapping of pore surfaces in the process of gasification, which can determine the peak reactivity of the reaction (Bhatia et al. 1980).

$$X = 1 - e^{-k_{RPM}t\left(1+\frac{\psi k_{RPM}t}{4}\right)}$$

Where ψ is a structural parameter using a reduced quantity that describes the particle's internal structure.

$$\psi = \frac{4\pi L_0(1-\epsilon_0)}{S_0^2}$$

Where S_0^2 is the pore's surface area per volume, S_0^2 is the pore length per volume and ϵ_0 is the solid porosity parameter. However, these values weren't available hence an alternate formula is used.

$$\psi = \frac{2}{2\ln(1-X_{max})+1}$$

Once Parameter is obtained, the reaction constant can be estimated similarly to the previous models. In determining the best fit model, the values will be fitted into the equation . The equation will help find the coefficient of determination (R) which will be used in determining the best fit model. Using the standard deviation formula , the overall goodness of the model will be determined.

$$R^2 = 1 - \frac{SS_{res}}{SS_{tot}} = 1 - \frac{\sum_1^N (X_{exp} - X_{model})^2}{\sum_1^N (X_{exp} - \overline{X})^2}$$

Where SS_{res} is the sum of squares of residuals from the experimental and empirical values while the SS_{tot} is the sum of squares from the experimental and the average values of char conversion.

$$SD = \sqrt{\frac{\sum (X_{exp} - X_{model})^2}{N-p}}$$

where X_{exp} and X_{model} are the conversion data from the experiment and each individual model and N is the number of data while p is the number of parameters fitted. After determining the best model for the sample, the activation energy was then determined using Arrhenius equation. The best kinetic model and parameters obtained were then compared to the other samples. This was all done using Microsoft Excel.

$$\ln\left(\frac{k_2}{k_1}\right) = \frac{E_a}{R}\left(\frac{1}{T_1} - \frac{1}{T_2}\right)$$

B. **Conversion Efficiency**
(Barrera, Umadhay, Canson, Larroder)

Photovoltaic (PV) panels are subject to extreme heat and radiation while exposed to sunlight. For sustainability reasons, organic bio-based Phase Change Materials (PCMs) are used to cool the temperature of the PV panel since they have a desired thermodynamic and kinetic criteria for low-temperature latent heat storage. This study aims to check the potential of bio-based phase change material which is the 1:7 mixture of rice bran wax to rice bran oil (RBW/RBO) in determining the conversion efficiency of the photovoltaic cells.

The wattages of the PV/PCM systems were computed using the equation of power which is the current multiplied by the voltage that was obtained using a multimeter. Efficiency was calculated and the gathered data was compared to the PV cell without PCM attached, and to the PV cell with paraffin wax.

Conversion Efficiency of the PV cell was determined using the following equation:

$$\eta = \frac{FF \times I_{sc} \times V_{oc}}{P_{in}}$$

Where V_{OC} was the open-circuit voltage, I_{SC} was the short-circuit current, FF was the fill factor, P_{in} was the power input and η was the efficiency. The Fill Factor (FF) was essentially a measure of the quality of the solar cell. It was calculated by comparing the maximum power (P_{MAX}) to the theoretical power (PT) that would be output at both the open-circuit voltage and short circuit current together.

$$FF = \frac{P_{max}}{P_T} = \frac{I_{MP} \cdot V_{MP}}{I_{SC} \cdot V_{OC}}$$

CONSTRUCTION

OVERVIEW

Geometric construction is the process of drawing a geometrical figure using geometrical instruments. This chapter discusses one of the techniques on how to construct a figure to determine whether the Golden ratio exists in the structures under study. The methods included in this chapter may be used as a reference to replicate similar studies.

A. Geometric

(Clement, Josue, Ledesma, Murga, Madriñan)

One of the two techniques for observing the Golden ratio in structures is geometric construction, where the ratio of the different measurements of the structure under study is taken. In this study, a spreadsheet was used for the automation of calculations.

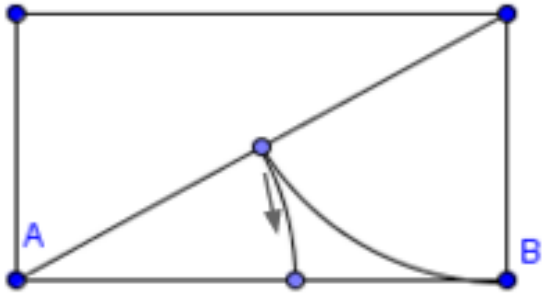

Figure 18*. Geometric construction.*

A line was partitioned to locate its golden section by first drawing a line with the length of AB. Next, the rectangle with the length AB and width AB/2 is drawn. A diagonal was drawn from A to the opposite corner of A.

Then, the width (AB/2) was then subtracted from the diagonal by drawing an arc with the width as the radius. The diagonal was then divided into two segments as a result of the intersection of the arc with the diagonal. Finally, the longer segment of diagonal was rotated onto the adjacent side, AB. The intersection point, C subdivides AB into the golden ratio. C is called the golden section of AB.

The figure was then scaled and overlaid on the scaled illustrations or blueprints of the structures under study to visually locate golden ratios.

DESIGN

OVERVIEW

Equipment design, in the absence of standardized equipment, is crucial in research methodology as it directly affects the results of the study and how data is interpreted. This chapter is a catalog of methodologies involving equipment and apparatus design. The following designs have been modeled from previous works of the same field but have been modified for feasibility and to better suit the purpose of their respective studies. Design heavily involves the kind of material used, the dimensions of the material, and in some cases, the chemical compositions of a particular layer.

A. Device

(Gurrea, Peregrino, Regalado, Salvador)

The core aspects of the design involve the utilization of 3 bubbling chambers. As CO2 is bubbled through the first solution, it reacts in the first chamber with Ca(OH)2 to initiate the carbon mineralization process and is then converted to CaCO3. However, since not all CO2 is expected to react, additional chambers have been added to allow the escaping CO2 to be sequestered and react again with the Ca(OH)2 filled chambers.

The design was also conceived through the aid of a professional mechanical engineer, Edgar Allan Vargas. The engineer was able to contribute mostly to the practicality of the device design rather than the chemical design behind the device. The extent of his contribution was mostly centered with regards to its feasibility to manufacture, its practicality, and changes in dimensions to facilitate the welding of stainless steel tubes.

A rectangular chamber was chosen for the sake of fabrication. Stainless steel is a relatively hard metal to bend and weld. Also, allowing for other geometrical shapes would have also meant an irregularly shaped device and would have made it bulkier. Rectangular shapes decrease the total space the device occupies. Hence, for our device, a rectangular chamber was chosen. To empty the Ca(OH)2 solution in the device, a

The design also includes input and output tubes to facilitate the flow of air. Some padding was placed between the roof of the device and the chamber so that it may be sealed airtight. The roof of the device is removable with nuts and bolts holding it together.

B. Assembly of Lens

(Ebojo, Magan, Dumalag, Larroder, Aban)

The concentrator photovoltaics requires a light source to be within the system's acceptance angle to achieve the highest output. A concentrator lens configuration was designed for a tandem III-V multi-junction solar cell in order to address this problem, improve the power output of the setup, and thereby reduce the need for a solar tracker.

The modified setup, Double Convex-Hemispherical lens (DCX-HSL), is composed of three lenses: the convex, Fresnel, and the hemispherical lens as shown in Figure 19. The convex lens was situated 10 cm above the multi-junction solar cell of the setup which is the topmost lens. The convex lens acts as the collector lens that collimates the beam of light from the sun to the next lens of the setup, the Fresnel lens. The concentrated light was distributed by the hemispherical lens on the surface of the solar cell for uniform irradiance distribution.

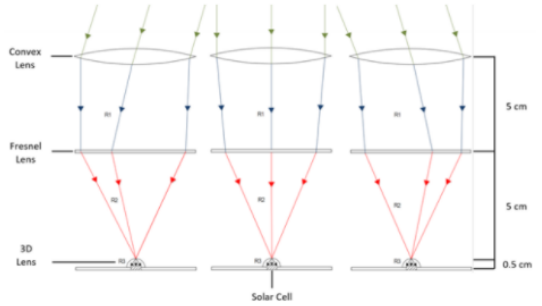

Figure 19. *Diagram of the compound convex-hemispherical setup*

A convex lens and hemispherical lenses were added to the optical system of the Fresnel lens setup. The convex lens was situated 10 cm above the multi-junction solar cell of the setup. The Fresnel lens was situated 5 cm on top of the multi-junction solar cell and concentrates the light on the solar cell. A hemispherical lens was situated on the solar cell for the distribution of light on the solar cell. The placements and specs of the lenses were optimized based on Köhler illumination where light from a certain range of angles is still redirected onto the surface of the solar cell. Köhler illumination is a method for generating an even illumination of the source on the object which in this case is the solar cell.

C. Column Design
(Bandiola, Galotera, Sampiano, Mediodia)

Before the columns were packed, they were washed with distilled water thrice and 10% nitric acid and were left to air-dry. They were stored in a 10% nitric acid wash bath overnight. Using a wooden rod, glass wool was packed inside the column up to a height of 2 cm. After making sure that that layer was flat, the adsorbent layer (rice husks for setup A; mango peels for setup B. An equal combination of rice husk and mango peels for setup C) was then poured inside the column until a 15 cm layer was formed. For combining the adsorbents in setup C, a 50:50 adsorbent ratio based on bed height was implemented, and the mixing process was performed by pouring the adsorbent inside a beaker and performing manual agitation. The adsorbent inside each column was weighed and was controlled for all replicates. Figure 20 shows the schematic diagram of the column setup. The sides of the column were tapped for an even distribution of the adsorbents. A final layer of glass wool with a height of 1 cm was placed on top of the setup in order to secure the adsorbent in place. As a primer, 100 mL of deionized water was passed through the column.

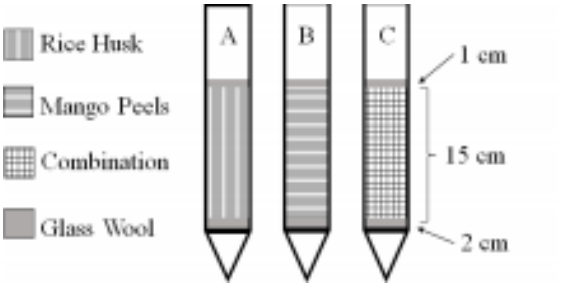

Figure 20*. The schematic diagram of the column setups is composed of a) rice husks only, b) mango peels only, and c) a combination of rice husks and mango peels.*

ELECTRONICS

OVERVIEW

Electronics deals with the design of circuits using transistors and microchips, and with the behavior and movement of electrons in any medium. This chapter discusses the different designs of Fresnel Lens, and Two Lens Setup. By varying measurements of length (spacing) and angles, these experimental setups were able to determine which of their proposed designs produces the highest power output.

A. Fresnel Lens Setup

Method A

(Barrios, Cortez, Herman, Larroder, Yu Jeco, Watanabe, Okada)

The Fresnel lens setup is comprised of a Fresnel lens mounted 5 cm above the solar cell, as shown in Figure 21. The solar cell is placed 5 cm under a Fresnel lens measuring 5 cm x 5 cm with a measured optical efficiency of 96.2% as measured using an irradiance meter and sourcemeter. Additionally, the lens has an estimated acceptance angle of 84.7 to 101.6°relative to the lens surface as measured with a laser pointer and a protractor.

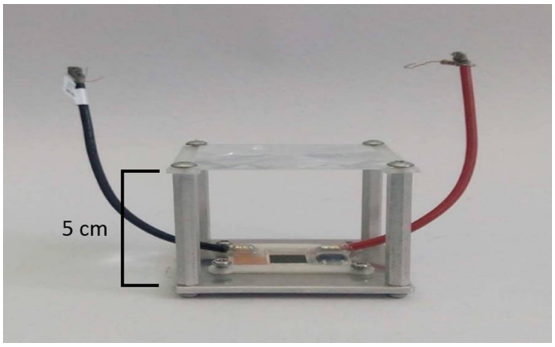

Figure 21. *The Fresnel lens setup with a Fresnel lens concentrator.*

Method B

(Ebojo, Magan, Dumalag, Laroder, Aban)

The concentrator photovoltaics requires a light source to be within the system's acceptance angle to achieve the highest output. A concentrator lens configuration was designed for a tandem III-V multi-junction solar cell in order to address this problem, improve the power output of the setup, and thereby reduce the need for a solar tracker.

For the theoretical modeling of the DCX-HSL setup, the software Edraw Max™ was utilized to create a light ray diagram. A diagram was created to have an expected result and view of how the setup will function when assembled. For the controlled setup, the Fresnel lens setup was used. It consisted of a solar cell and the Fresnel lens which served as the primary concentrator. In this setup, the Fresnel lens was situated 5cm above the solar cell as shown in Figure 22.

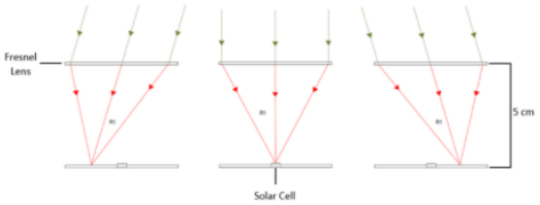

Figure 22. *Diagram of the Fresnel lens setup.*

The Fresnel lens setup is composed of one Fresnel lens and a multi-junction solar cell. The solar cell was secured on the aluminum backplate with the solar cell holder and screws. The spacers were then screwed to the aluminum backplate with the washers between the aluminum backplate and screws. The lens holders were screwed to the spacer, then the Fresnel lens was lodged into place and was secured using screws. The Fresnel lens in this setup was placed 5 cm above the multi-junction solar cell as shown in Figure 21. It served as the primary concentrator for the setup.

B. Two-lens setup

(Barrios, Cortez, Herman, Larroder, Yu Jeco, Watanabe, Okada)

A convex lens with a diameter of 5 cm, a focal length of 10 cm, and an estimated acceptance angle of 83.7 to 97.5° relative to the lens surface was selected. It was mounted at a fixed height of 5 cm above the Fresnel lens using the iron stand and iron clamp, as shown in Figure 23.

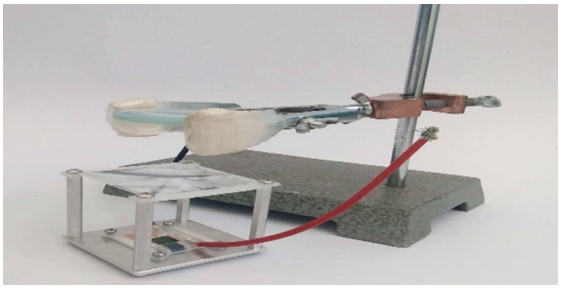

Figure 23*. The two-lens system with a convex lens as primary concentrator located 5 cm above the Fresnel lens secondary concentrator.*

The specific measurements for the lens installation were calculated using the Lens-Maker's equation (1), where the dimensions were selectively aimed at having the focal point of the two-lens system placed exactly on the solar cell's surface. f1 and f2 represent the focal lengths of the convex and Fresnel lenses, respectively, d represents the distance between the two lenses, and f represents the composite focal length of the entire lens system.

$$\frac{1}{f} = \frac{1}{f_1} + \frac{1}{f_2} - \frac{d}{f_1 f_2}.$$

EVALUATION

OVERVIEW

Evaluation provides a systematic method to determine the efficacy of a certain quality or process. This chapter discusses experimental methods for evaluating the plastic degradation of three types of plastics and the absorbency of a hydrogel, a superabsorbent polymer. Evaluating the qualities of different materials may support future studies on product design, and later on manufacturing.

A. Plastic Degradation (% Weight Loss)
(Canja, Hilis, Galan, Jolito)

Plastics are known for being durable materials while still maintaining a low cost of production. It is a very important material for commercial use all over the world. However, due to the lack of a reliable method of disposal, the risk of plastic pollution is steadily increasing throughout the years. This study aims to isolate and extract bacteria from the Iloilo City Engineered Sanitary Landfill, in Mandurriao, Iloilo City, and to assess their biodegradation potential on LDPE (Low-density polyethylene), HDPE (High-density polyethylene), and PET (Polyethylene terephthalate).

The three different types of plastics (PET, LDPE, HDPE) were cut into strips having dimensions of 2cm x 2cm with 3 times replication for each plastic in each set-up. They were sterilized in 70% ethanol for 30 minutes, washed with distilled water, and subsequently dried in an incubator at 60° C for 24 hours. Afterward, plastics were put into a silica gel containing desiccator for 24 hours for total water evaporation. The initial dry weight of plastic was measured with an analytical balance (Kyaw et al., 2012).

After bacterial culture, three set-ups were made. Colonies were selected based on their morphological characteristics: form, elevation, and margin. The first being the medium inside the Petri dish where Bacteria 1 was cultivated with the three types of plastic strips (HDPE, LDPE, and PET) having each type of test plastics in triplicates.

The second setup was the medium with Bacteria 2, and the same was done for this setup. The two colonies were distinguished using the nutrient agar eosin methylene blue agar (EMB) and mannitol salt agar (MSA) as shown in Plate 1. The last set-up is the control, which was maintained with polyethylene strips in the microbe-free medium. Pre-weighed strips of sterilized plastics of each type were aseptically transferred to the Petri dish containing mineral salt medium (MSM) and inoculated with the bacteria to be tested.

Plate 3-4. *Bacterial strains EMBP2A and MSAP2A for incubation.*

Triplicates were maintained for each type of plastic and were left on the incubator. After 10 days, the plastic discs were collected and washed thoroughly using distilled water. They were then dried in a hot air oven at 50°C overnight for at least 10 hours and were weighed for final dry weight. The percentage weight loss was calculated using the formula below (Usha et al., 2011).

$$\text{Weight loss } (\%) = \frac{\text{initial weight} - \text{final weight}}{\text{initial weight}} x100$$

B. **Superabsorbent Polymer Absorbency**

(Gerona, Sorongon, Remaneses)

The absorbency of the hydrogel or the volume of water the polymer can absorb was determined as follows: 1 g of hydrogel was immersed in 200 mL distilled water at room temperature (30°C) and the weight was measured every hour for five hours.

The tea bag was allowed to drain for 10 min or until the excess water stopped dripping. The equation for the swelling capacity or absorbency is as follows: Absorbency = (W2 − W1)/W1 where W1 and W2 represent the weight of the dry polymer and the swollen gel, respectively. The rate of absorption was obtained by determining the absorbance at consecutive time intervals.

FIELD TESTING

OVERVIEW

Field testing is an important procedure in product research and development as it is pertinent in gauging whether the design of the product is effective in its target environment. This then refines the scope of the research and the specifications of the product. In this chapter, two modified and controlled setups of field testing involving lens and PVC with bio-based PCM are cataloged; both of which required sunlight and had taken place at Philippine Science High School - Western Visayas.

A. Lens

(Ebojo, Magan, Dumalag, Larroder, Aban)

The concentrator photovoltaics requires a light source to be within the system's acceptance angle to achieve the highest output. A concentrator lens configuration was designed for a tandem III-V multi-junction solar cell in order to address this problem, improve the power output of the setup, and thereby reduce the need for a solar tracker.

The Fresnel lens (controlled) setup and Double Convex-Hemispherical lens (modified) setups were tested on the rooftop of the Student Learning Resource Center (SLRC) building located at Philippine Science High School - Western Visayas. The modified and controlled setups were placed on a table and the angle of the controlled and modified setups was adjusted to 0 degrees in reference to the ground using the built-in compass app of Apple to make sure it was flat as shown in Figure 24. Voltage, current, solar irradiance, and the time of data gathering, were recorded during the outdoor data gathering.

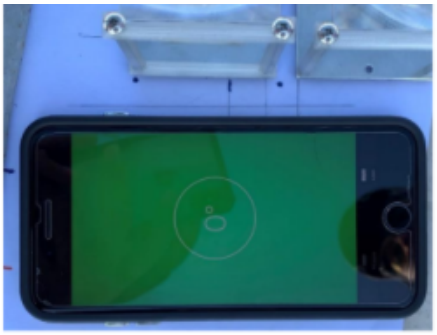

Figure 24. *Angle of the modified and controlled setup in reference to the ground.*

Two multi-testers were used for measuring the voltage and the current while a solar irradiance meter was used to measure the solar irradiance for two setups. The multimeters were calibrated by setting the two to the highest resistance range option and the red and black probes that were connected to the multimeter were touched together until the reading on the multimeters displayed "0 ohms". After calibration, the measuring devices were used to measure the parameters. The measurements were repeated until three of the values have a difference equal to or less than one on the rightmost significant digit for the reliability of the data. This process was repeated every hour starting from 6:15 am until 5:15 pm. Weather conditions such as the cloud cover were recorded and were taken into consideration during the data gathering because it may affect the data gathered.

B. PVC with Bio-based PCM

(Barrera, Umadhay, Canson, Larroder)

Photovoltaic (PV) panels are subject to extreme heat and radiation while exposed to sunlight. For sustainability reasons, organic bio-based Phase Change Materials (PCMs) are used to cool the temperature of the PV panel since they have a desired thermodynamic and kinetic criteria for low-temperature latent heat storage. This study aims to check the potential of bio-based phase change material which is the 1:7 mixture of rice bran wax to rice bran oil (RBW/RBO) in determining the conversion efficiency of the photovoltaic cells.

From the simulation result of Indartano et al. (2015), the optimum thickness of the PCM was at 80 mm. The thicker the PCM mounted on the solar module is, the greater the drop in temperature experienced by the solar modules, especially at the backside of the solar module. This was due to the thickness of the PCM being proportional to the total volume of PCM. The larger the volume of PCM, the more time it needs to melt all the PCM. The aluminum tube was used for the purpose of heat collection, removal, and possible recovery. Two fabricated rectangular containers made of aluminum held the PCMs; one for the rice bran wax and rice bran oil mixture and one for the paraffin wax. The more contact of the material to a metal, the greater the thermal conductivity, thus, spreading the heat more evenly throughout the PCM (Hasan et al. 2010).

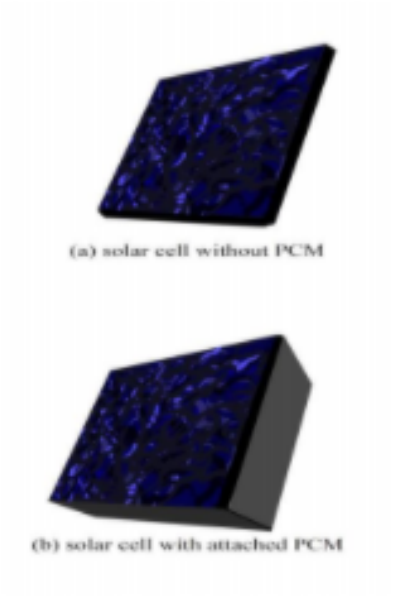

Figure 25*. PV cell Schematics (not drawn to scale)*

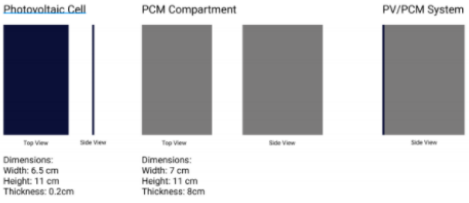

Figure 26*. The dimensions and components of the PV cell and schematics of PV with PCM attached to it (not drawn to scale).*

The containers were placed under the PV module to create the PV/PCM system. K-type thermocouples were attached to the back of the PV cell and to the PCM to monitor temperature changes.

The actual testing of the PV cell with and without attached phase change materials was performed in the Smart Classroom 2 of Philippine Science High School- Western Visayas Campus. A box made of illustration board 21 cm high, 9 cm wide, and 15 cm long was constructed to act as a dark room for the PV cell and to hold in place the xenon lamp. The temperature, current, and voltage were measured every 15 minutes using thermocouples and a multimeter. The open-circuit voltage (VOC) and short circuit current (ISC) were first measured by connecting the PV cell to an equivalent circuit with a single diode and series resistance mode, under the illuminated light of a xenon lamp. The VOC was measured when the current in the circuit is equal to zero while the short circuit current was measured when the voltage in the circuit is equal to zero. Only parameters VOC and ISC were measured due to the unavailability of specialized equipment for voltage sweep analysis used in determining the actual measurement of maximum power output (PMAX) in the PV cell. Instead, the actual values of the two were used and derived to calculate the efficiency, together with its underlying parameters-- fill factor (FF) and (PMAX). The voltage and current of the PV cells were simultaneously measured using a multimeter. The temperature of the PCM and the back surface of the PV cell were also measured simultaneously. The value of the solar irradiance was also measured every 15 minutes using the solar irradiance meter.

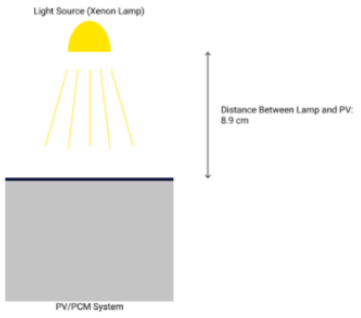

Figure 27*. Set-up with the distance between Xenon lamp and PV/PCM*

MATERIAL TESTING

OVERVIEW

This chapter provides different methods of determining quantitative characteristics of a raw material and a commercial product. This category discusses three mechanical properties, i.e. tensile strength, tear resistance, and stiffness, which are important for textiles and bag-making, and an optical property, reflectivity, which may be used for urban planning and design. These research investigations promote studying locally-available materials for their potential uses and possible commercial value.

A. **Tensile Strength**
(Aguilar, Lignig, Togonon, Brana, Tanoy)

The tensile test was performed using the Universal Testing Machine(UTM) Instron Model 1000 by pulling the samples under tension until breakage. The data for the results were then calculated and derived using the maximum force and extension at break displayed by the machine. The standard used was ASTM D828-97(2002): Test Method for Tensile Properties of Paper and Paper Board Using Constant-Rate-of-Elongation Apparatus, using Instron Model 1000 Universal Testing Machine(UTM). This standard was used as procedure reference only for the test and not a specific test standard for leaf sheaths or canvas.

B. **Tear Resistance**
(Aguilar, Lignig, Togonon, Brana, Tanoy)

For the tear test, the machine used was Elmendorf Model 60-100 Tear Tester, and the standards used were ASTM D689-"Test Method of Internal Tearing Resistance of Paper" and TAPPI T414-"Internal Tearing Resistance of Paper (Elmendorf Type)". The standards were used as procedure reference only and not a specific standard test for leaf sheaths or canvas. The test conditions were consistent throughout the test, with 26.7℃ at 44% relative humidity. The average tearing force in grams was calculated by multiplying 16 the scale reading of the machine, and then dividing by the number of plies(from the ASTM and TAPPI standards used).

C. **Tear Resistance**
(Aguilar, Lignig, Togonon, Brana, Tanoy)

For the tear test, the machine used was Elmendorf Model 60-100 Tear Tester, and the standards used were ASTM D689-"Test Method of Internal Tearing Resistance of Paper" and TAPPI T414-"Internal Tearing Resistance of Paper (Elmendorf Type). The standards were used as procedure reference only and not a specific standard test for leaf sheaths or canvas. The test conditions were consistent throughout the test, with 26.7℃ at 44% relative humidity. The average tearing force in grams was calculated by multiplying 16 the scale reading of the machine, and then dividing by the number of plies(from the ASTM and TAPPI standards used).

D. **Reflectivity**
(Apdon, Frange, Salistre, Larroder)

A Samsung J7 Prime with a 13-megapixel camera that can run the Albedo: Reflectance AppTM was used for the study. The application works by comparing the image of the sample with an image of a photographer's gray card as a calibrator (which has a known albedo of 0.18). Since the objective of the study is to determine if there is an increase in albedo due to the addition of *Placuna placenta*, the absolute albedo readings are not necessary but rather, albedo testing of each slab must be at identical background conditions to have the same basis for the application to determine the relative albedo values.

MEASUREMENT

OVERVIEW

Measurement is the quantification of the various attributes of an object. This section will deal with the measurement of thermophysical properties, particularly that of rice bran wax and rice bran oil mixture. The method outlined in this section may be adapted to substances of similar properties.

A. Thermophysical Properties

(Barrera, Umadhay, Candon, Larroder)

Photovoltaic (PV) panels are subject to extreme heat and radiation while exposed to sunlight. For sustainability reasons, organic bio-based Phase Change Materials (PCMs) are used to cool the temperature of the PV panel since they have a desired thermodynamic and kinetic criteria for low-temperature latent heat storage. This study aims to check the potential of bio-based phase change material which is the 1:7 mixture of rice bran wax to rice bran oil (RBW/RBO) in determining the conversion efficiency of the photovoltaic cells.

The thermophysical properties of the rice bran wax and rice bran oil mixture which are the melting point, the heat of fusion and supercooling/subcooling, latent heat of fusion, and heat capacity were measured using differential scanning calorimetry (DSC) analysis. The samples were taken to the University of the Philippines-Visayas Miag-ao for the DSC analysis. One gram of the rice bran mixture sample was heated and the changes in its heat capacity were tracked as changes in the heat flow. This allowed the detection of transitions such as melting point and phase changes. In DSC, the 1:7 ratio of rice bran wax to oil mixture was heated at a constant rate. The latent heat of fusion of the material was measured by using the area below the peak and melting temperature was measured by the tangent at the point of maximum slope on the face part of the peak.

The samples were held for 1 minute at 15 °C. It was heated at a linear rate of 10°C/min from 15°C to 36°C in a nitrogen atmosphere. The differential scanning calorimetry (DSC) is to determine if the sample was starting to melt. It was held again for 2 minutes at 36°C and was heated from 36°C to 40°C at 1°C/min before it was held for 2 minutes to check if the samples were completely melted. It was heated again at 40°C to 500°C with a heating rate of 10°C/min before it was cooled down from 500°C to 40°C at 20°C/min. The percentage of the thermophysical properties was determined by extrapolating the slopes of the thermographic curves above and below the inflection temperature. The intersection of these slopes allowed the determination of the weight loss and thus the percentage of the components and the reactions that were present.

Data on the thermophysical properties of rice bran wax and rice bran oil mixture were compared to the established thermophysical properties of paraffin wax as it is the most common type of PCM that is being attached to PV cells for cooling. The basis of the thermophysical properties of paraffin wax was acquired from the research of Kavitha and Arumugam (2013). Paraffin wax is an organic PCM that has been tested to improve PV panel efficiency and it was the most common PCM that can be used in lowering the PV cell temperature (Hasan et al. 2010; Wei et al. 2017; Cellura et al. 2008).

PROCUREMENT

OVERVIEW

Procurement is the act of acquiring materials or values needed to proceed with the research design. This chapter discusses how measurements of a structure were obtained through various methods, and how Phase Change Materials (PCM) were selected according to established standards. It is important to be critical in the procurement stage as it would affect the analysis in the later part of the study.

A. Measurements

(Clement, Josue, Ledesma, Murga, Madriñan)

In using the measurement of structures as a subject of the study, acquiring blueprints or plans of the structure is the most common method. Should there be no available blueprints or measurements of the whole structure or certain parts of the structure needed, manual measurement of the structure with the aid of a laser distance measuring device or tape measure can be done.

The relatively longer lengths in this study were measured with the laser device while the lengths that were hard to get using this device were measured with tape measure. The measurements in meters were taken at least three times and then averaged. Since the laser measurement device has an area for error of 1.5 mm, then each measurement obtained should be placed in a range of ±1.5 mm. However, the value 0.0015 was too small to be significant in collecting measurements because the measurements obtained have been rounded off to two decimal places.

B. Bio-Based Phase Change Materials (PCM)

(Barrera, Umadhay, Candon)

Photovoltaic (PV) panels are subject to extreme heat and radiation while exposed to sunlight. For sustainability reasons, organic bio-based Phase Change Materials (PCMs) are used to cool the temperature of the PV panel since they have a desired thermodynamic and kinetic criteria for low-temperature latent heat storage.

This study aims to check the potential of bio-based phase change material which is the 1:7 mixture of rice bran wax to rice bran oil (RBW/RBO) in determining the conversion efficiency of the photovoltaic cells.

The criteria for PCM selection is broadly based on the following physical, thermal and chemical properties. According to Xu et al. (2017) first, the phase change temperature of this material should satisfy the operating temperature range of the latent heat storage energy system. A PCM with an easily adjustable melting point would be a necessity as the melting point is the most important criterion for selecting a PCM for passive solar applications (Farid et al. 2004). Second, the PCM should possess high latent heat of fusion and large specific heat, to ensure the high storage density of the system. Lastly, the material is required to have high thermal conductivity in order to achieve high discharge power.

According to the Certificate of Analysis, the melting point of the rice bran oil was only 15°C. The phase change temperatures of rice bran oil, which is a fatty acid, could be adjusted by mixing fatty acids in a suitable proportion. A more appropriate solution was to utilize another type of PCM with a more reasonable melting point that was suitable for the application.

One of the ways on how the melting point of the PCM could increase was to adjust its characteristics, or by mixing it with other types of PCM with a lower melting point until the desirable melting point was achieved. Rice bran wax has a melting temperature of 79°C (Kramer 2016). It was

then mixed with rice bran oil to create a mixture that will have a melting point higher than the rice bran oil but lower than that of the rice bran wax. There were seven mixtures having different ratios of rice bran wax to rice bran oil in terms of volume, which were 1:1, 1:2, 1:3, 1:4, 1:5, 1:6, and 1:7 respectively. The rice bran wax was melted first using the hot plate and rice bran oil was added to it while it was being heated and was mixed and stirred using a stirring rod. Different ratios created mixtures with differences in the melting point. It was found out that the mixture with the 1:7 ratio was the most suitable for the study since its melting temperature is in line with the operating temperature of the PV cell.